An alternative to least-squares imaging using data-domain matching filters

A. Khalil, H. Hoeber, G. Roberts and F. Perrone, CGG*

Summary

Posing migration as an inverse or a least-squares problem can improve the quality of imaging. This class of technique can resolve illumination issues and improve focusing. Standard iterative least-squares imaging can be expensive and results are often compromised. We present a procedure using matching filters operating in data-space rather than image-space. Effective inversion results are demonstrated on synthetic and real data.

Introduction

Seismic migration or imaging maps energy recorded at the surface back to its correct location in the subsurface. A successful migration algorithm generates an image that represents the geological reflectivity of the earth. Essentially, this is an inversion process; however, most imaging algorithms are formulated as adjoint operators rather than true inverses (Claerbout, 1992). This may lead to non-uniform illumination, imaging artefacts and reduced resolution (Nemeth et al., 1999).

Least-Squares Migration (LSM), for example Zhang et al. (2013), solves for an image that resembles seismic data when de-migrated. LSM is typically implemented as an iterative procedure that minimizes the difference between observed and modelled data. This requires multiple iterations to converge and can be expensive. Migration deconvolution schemes (MD), for example Hu et al. (2001), provide alternative solutions by estimating and applying de-blurring filters that mimic the effect of the inverse Hessian operator. Both approaches are theoretically equivalent but due to the different implementation, performance can be different. A comparison between the two approaches is found in Yu and Schuster (2003).

We present a methodology using matching filters similar to Guitton (2004). The filters are derived and applied in data-domain rather than image-domain. For ease we will refer to it data-domain deconvolution. This gives rise to a new class of LSM solutions based on generalized inverses. We demonstrate that the new approach provides a better solution in under-illuminated regions of the image, for example around steeper reflectors.

Theory

The LSM goal is to update a migrated image in order to match the observed data after demigration. The solution is found by minimizing the cost functional

$$E = \left\| \mathbf{d} - \mathbf{L}\mathbf{r} \right\|^2 , \tag{1}$$

where $\mathbf{d}$ is the observed input data, $\mathbf{L}$ is the de-migration or modelling operator and $\mathbf{r}$ is the least-squares solution i.e. the image or reflectivity model. The standard least-squares solution is given by

$$\mathbf{r} = \left(\mathbf{L}^T\mathbf{L}\right)^{-1}\mathbf{L}^T\mathbf{d} , \tag{2}$$

where $\mathbf{L}^T$ is the adjoint of the de-migration operator i.e. the migration operator.

In Equation 2, the operator $\left(\mathbf{L}^T\mathbf{L}\right)^{-1}\mathbf{L}^T$ acts as a generalized inverse of $\mathbf{L}$; however it is not the only choice. The theory of generalized-inverses provides other alternatives (Ben-Israel and Greville, 2004, Golub and Van Loan, 1996). In the context of seismic imaging, we propose to use operator $\mathbf{L}^T\left(\mathbf{L}\mathbf{L}^T\right)^{-1}$ instead, giving rise to the solution

$$\mathbf{r} = \mathbf{L}^T\left(\mathbf{L}\mathbf{L}^T\right)^{-1}\mathbf{d} . \tag{3}$$

Both Equations 2 and 3 provide inverse formulations for the demigration operator. Equation 2 is more suited to over-determined problems while Equation 3 is more suited to under-determined ones.

In a complicated geological setting, the subsurface encompasses a range of well illuminated areas and regions which are less penetrable leading to under-illumination. The imaging problem can be viewed as an entirety of over- and under-determined local smaller problems. Clearly, areas with poor illumination suffer most - for example, subsalt regions and around steeper reflectors. We argue that Equation 3 can provide a better image in these instances.

We propose to solve Equation 3 using a methodology similar to Guitton's (2004). However, we operate in the data-space rather than in the image space.

The operator $\left(\mathbf{L}\mathbf{L}^T\right)^{-1}$ is approximated by filters that match the de-migrated image to the original data; the matching operator is then applied to the input data and it is then re-migrated:

$$\mathbf{r} = \mathbf{L}^T\mathbf{P}\mathbf{d} , \tag{4}$$

where $\mathbf{P}$ is the matrix form of the non-stationary filters given by minimizing $f(\mathbf{p}) = \left\| \mathbf{d} - \mathbf{p} * \tilde{\mathbf{d}} \right\|^2$ and $\tilde{\mathbf{d}} = \mathbf{L}\mathbf{L}^T\mathbf{d}$.

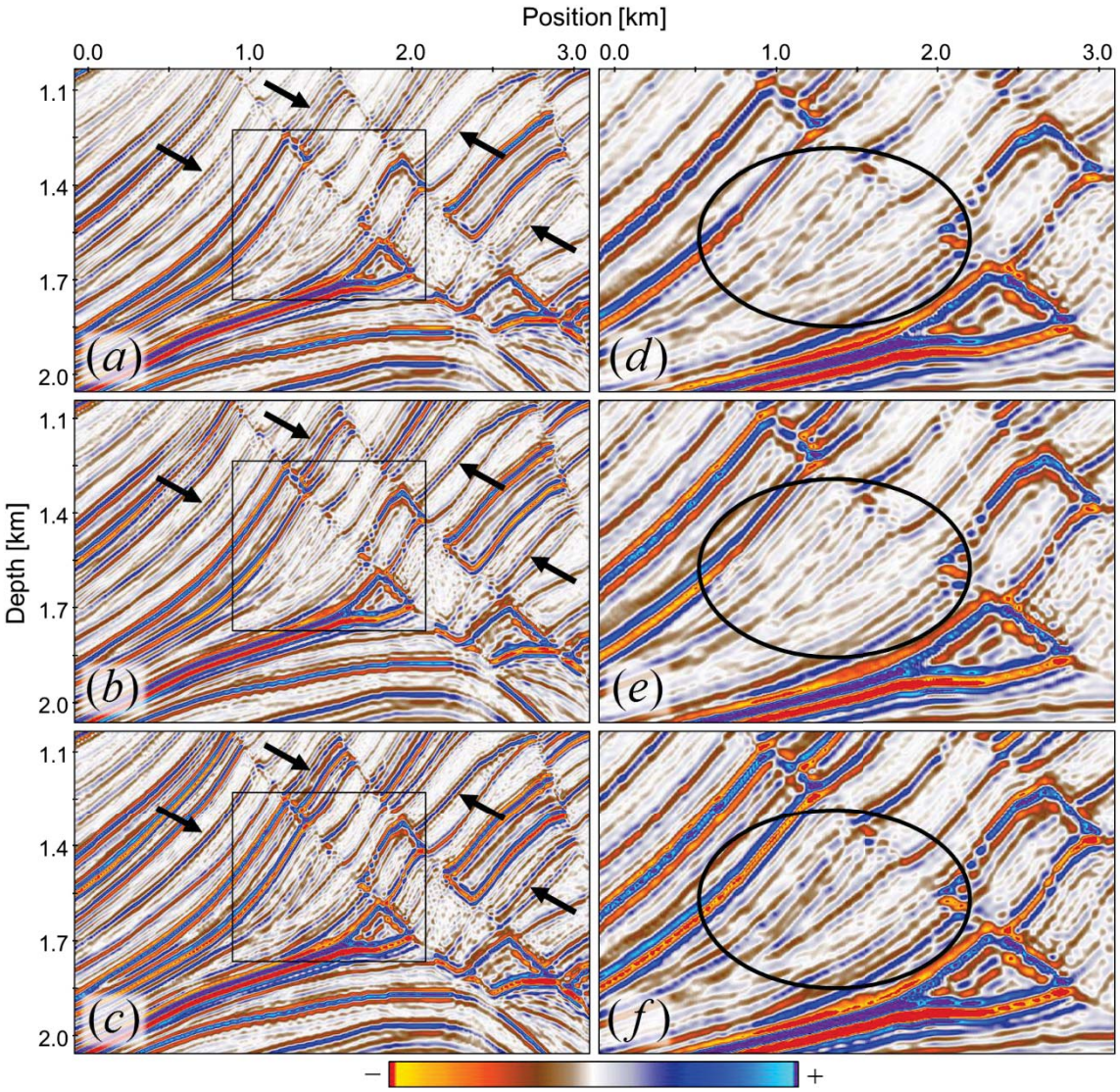

Figure 1: Reverse time migration of the Marmousi dataset. (a) standard migration (b) image-domain deconvolution (c) data-domain image deconvolution (d) Zoom in of the standard migration (e) Zoom in of the migration domain deconvolution (f) Zoom in of the data-domain deconvolution

Marmousi RTM example

Three Reverse Time Migrations (RTM) of the Marmousi dataset are shown in Figure 1. Due to incomplete illumination, steeper dips suffer the most in the standard migration (top). Events are fainter and less focused when compared to flatter events. The image-domain deconvolution approach as described by Guitton (2004) (middle) and the data-domain deconvolution described here (bottom) improve the illumination and focusing at steeper reflectors as well as reduce artefacts. The data-domain deconvolution method provides an improved outcome. The energy of the reflectors is more homogenous and matches those of the true reflectivity model. Zoomed displays of the section highlight an imaging artefact in the standard migration. The artefact is reduced by the image-domain and the data-domain deconvolutions. The data-domain approach further focuses underlying real reflectors and improves their definition.

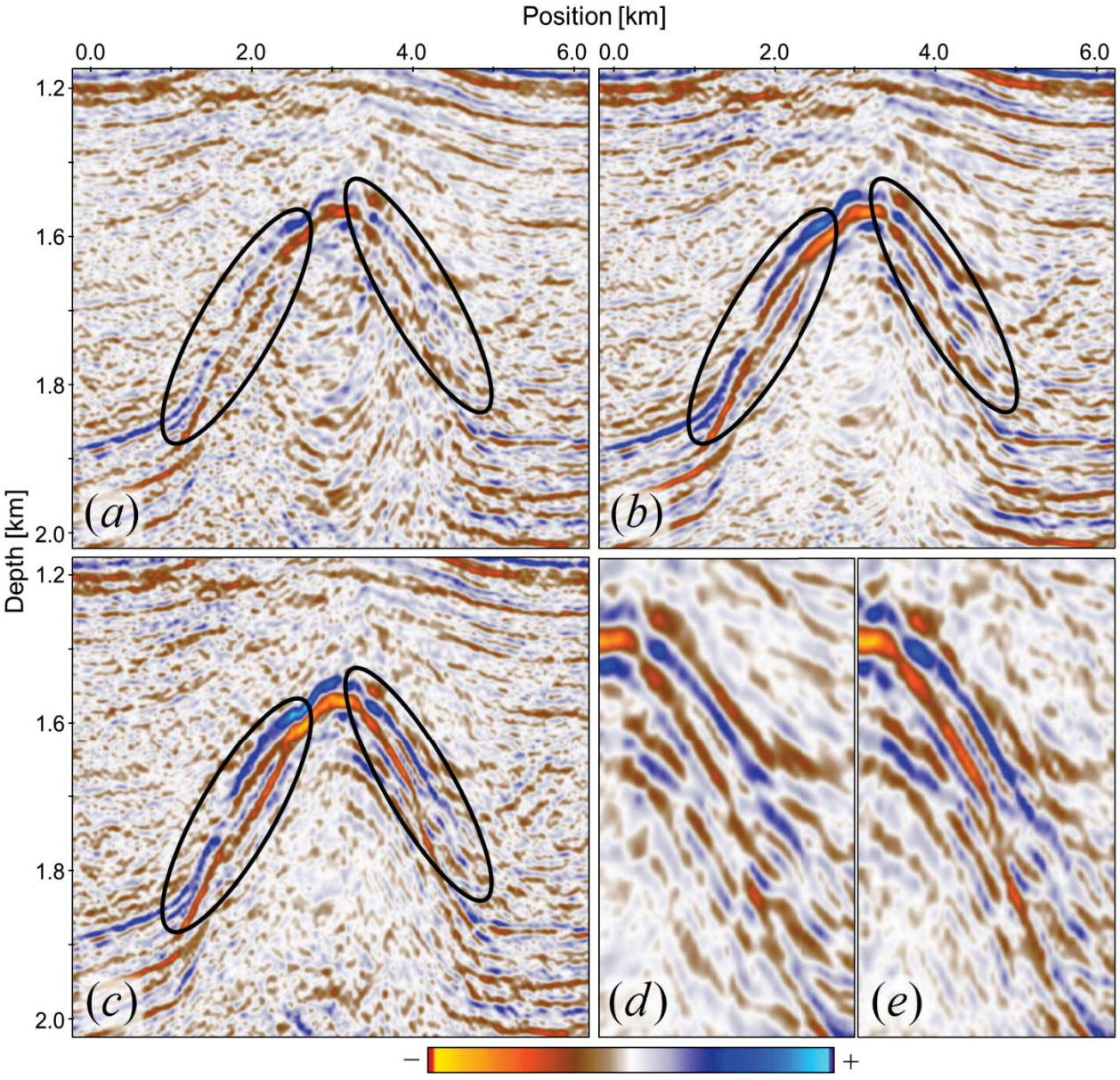

Figure 2: A single offset class migrated with Kirchhoff (a) standard migration (b) image-domain deconvolution (c) data-domain deconvolution (d) Zoom-in of the image-domain deconvolution (e) Zoom-in of the data-domain deconvolution

A North Sea Kirchhoff example

Figure 2 shows the migrated result of a single offset class from a North Sea dataset. The salt flanks from the standard migration (Figure 2a) are heavily distorted by imaging artefacts. The image is improved by the image-domain deconvolution scheme (Figure 2b). The data-domain deconvolution boosts the improvement further. The flanks are much better focused and easier to interpret. Zoomed in displays on the right salt flank (Figures 2d and 2e) demonstrate the improvement in focusing and continuity of the data-domain scheme.

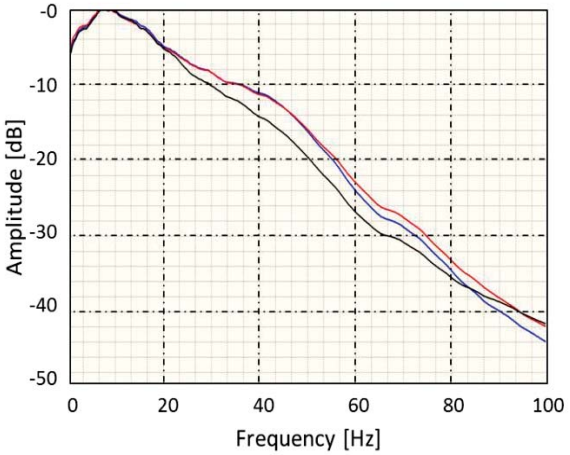

Figure 3: Amplitude spectra from different migrations. Black lines show the spectra from the standard migration, blue lines show the image-domain deconvolution results and red lines show the data-domain results.

Figure 3 shows extracted amplitude spectra for the three approaches. The two deconvolution approaches extend the bandwidth as expected from least-squares-migration-type algorithms.

A North Sea RTM example

Figure 4 shows the result of data-domain deconvolution on a reverse-time migrated North Sea dataset. Standard RTM results are shown for comparison (top figure). Steeper events receive less illumination and are degraded with respect to flatter reflectors. Resolution, definition and amplitudes are affected. Using this data-domain deconvolution technique (bottom figure), Overall imaging is significantly improved. Flank definition is greatly enhanced and the image is better focussed. The technique helps in compensating for these illumination issues and providing an overall better quality image.

Conclusions

A new approach to least-squares migration is presented. The method is formulated in a way similar to image deconvolution techniques but operates in the data domain. Compared to its image-domain equivalent, it delivers better imaging and focusing around under-illuminated regions. The method requires only a single extra migration and a single de-migration.

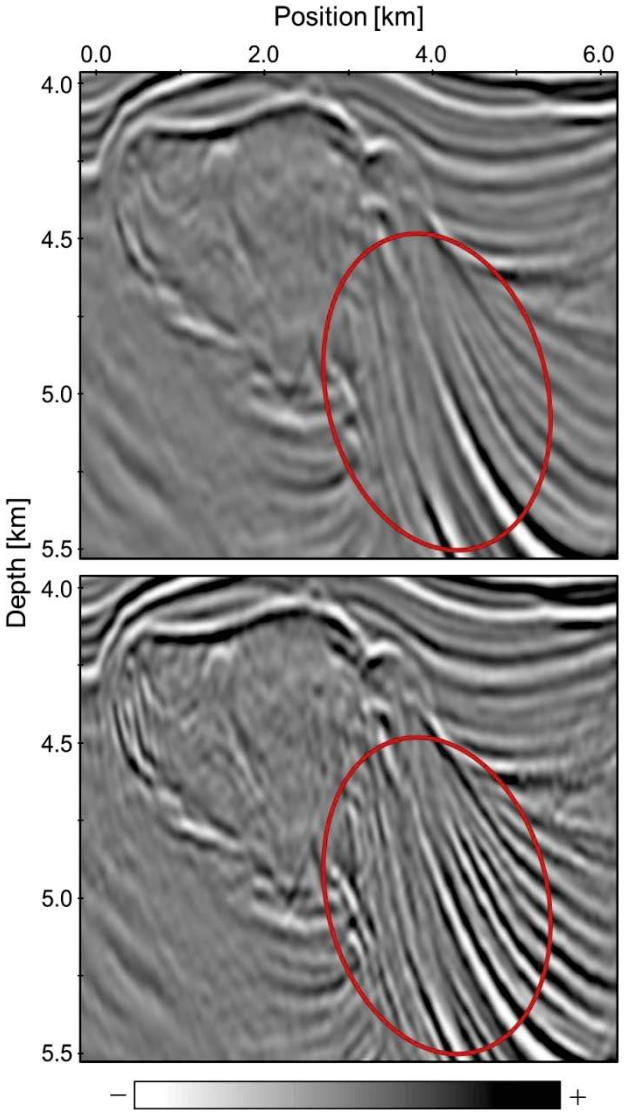

Figure 4: RTM migration of a North Sea dataset. (Top) Standard migration (Bottom) Data-domain deconvolution.

Acknowledgments

The authors would like to thank CGG for permission to publish this work and multi-client-new-ventures for permission to show the real data examples, and IFP for the Marmousi model.

EDITED REFERENCES

Note: This reference list is a copyedited version of the reference list submitted by the author. Reference lists for the 2016 SEG Technical Program Expanded Abstracts have been copyedited so that references provided with the online metadata for each paper will achieve a high degree of linking to cited sources that appear on the Web.

REFERENCES

Ben-Israel, A., and T. N. E. Greville, 2003, Generalized inverses: Theory and applications, 2nd ed.: Springer.

Claerbout, J. F., 1992, Earth Soundings Analysis: Processing versus Inversion: Blackwell Scientific Publications.

Golub, G., and C. van Loan, 1996, Matrix computations, 3rd ed.: The Johns Hopkins University press.

Guitton, A., 2004, Amplitude and kinematic corrections of migrated images for non-unitary imaging operators: Geophysics, **69**, 1017–1024, http://dx.doi.org/10.1190/1.1778244.

Hu, J., G. Schuster, and P. Valasek, 2001, Poststack migration deconvolution: Geophysics, **66**, 939–952, http://dx.doi.org/10.1190/1.1444984.

Nemeth, T., C. Wu, and G. T. Schuster, 1999, Least-squares migration of incomplete reflection data: Geophysics, **64**, 208–221, http://dx.doi.org/10.1190/1.1444517.

Yu, J., and G. T. Schuster, 2003, Migration deconvolution versus least squares migration: 73rd Annual International Meeting, SEG, Expanded Abstracts, 1047–1050.

Zhang, Y., L. Duan, and Y. Xie, 2013, A stable and practical implementation of least-squares reverse time migration: 83rd Annual International Meeting, SEG, Expanded Abstracts, 3716–3720, http://dx.doi.org/10.1190/segam2013-0577.1.